Technologies for Non-Destructive Evaluation of Surfaces and ThinCoatings

NAG 1-1814

3/15/97 - 3/14/98

FINAL REPORT

Dr. Dennis M. Manos and Dr. Christopher Welch
The College of William & Mary
P.O. Box 8795
Williamsburg, VA 23187-8795

NAG1-1814

Technologies for Nondestructive Evaluation of Surfaces and Thin Coatings

Final Report

1 Introduction and Overview

The effort included in this project included several related activities encompassing basic understanding, technological development, customer identification and commercial transfer of several methodologies for nondestructive evaluation of surfaces and thin surface coatings. Consistent with the academic environment, students were involved in the effort working with established investigators to further their training, provide a nucleus of experienced practitioners in the new technologies during their industrial introduction, and utilize their talents for project goals.

As will be seen in various portions of the report, some of the effort has led to commercialization. This process has spawned other efforts related to this project which are supported from outside sources. These activities are occupying the efforts of some of the people who were previously supported within this grant and its predecessors.

The most advanced of the supported technologies is thermography, for which the previous joint efforts of the investigators and NASA researchers have developed several techniques for extending the utility of straight thermographic inspection by producing methods of interpretation and analysis accessible to automatic image processing with computer data analysis. The effort reported for this technology has been to introduce the techniques to new user communities, who are then be able to add to the effective uses of existing products with only slight development work. In a related development, analysis of a thermal measurement situation in past efforts led to a new insight into the behavior of simple temperature probes. This insight, previously reported to the narrow community in which the particular measurement was made, was reported to the community of generic temperature measurement experts this year. In addition to the propagation of mature thermographic techniques, the development of a thermoelastic imaging system has been an important related development. Part of the work carried out in the effort reported here has been to prepare reports introducing the newly commercially available thermoelastic measurements to the appropriate user communities. This presentation represents culmination of an effort which was

initiated under a predecessor of this grant long before the measurement was commercially available. The availability of the full-field synchronous analysis of thermal data has opened opportunities for synchronous techniques which can extend the sensitivity of thermographic measurements by imposing suitably configured periodic heating stimuli. One such technique has been used in a related "daughter" project for measurement of thickness of a thin coating, such as paint. Another application, again now part of a separate project, involves using the full-field synchronous demodulation technique in visible light to obtain images of photoelastic responses at sensitivities far below a single fringe. At present, the College of William and Mary is the only organization outside of NASA which has this capability operational in visible light. The separate project, discussed below as related work, has the ambitious goal of developing an industrially useful full-field stress separation from a combination of thermoelasticity and photoelasticity.

The effort in Optically Stimulated Electron Emission (OSEE) this year has been directed primarily towards producing a hand-held instrument for potential commercial use, and it has been directed and executed entirely within the engineering development activity in the Nondestructive Evaluation Science Branch of NASA Langley Research Center. Efforts under this grant have related to this project in an advisory capacity. Other efforts, discussed below, have related to education and the identification of possible users of the technology. As part of this effort, the laboratory OSEE system has been relocated to the College of William and Mary and placed in operation there.

The effort in scintillator analysis, to characterize the absorption and luminescence characteristics of glass fibers doped with terbium, is expected to come to a conclusion during the current grant period. A presentation on the results has been given at a national scientific meeting.

2 Activities and Accomplishments

The work described in this section, while addressing the entire project, highlights the final year of the effort. Previous reports, submitted on an annual basis, have covered some aspects of the work more extensively.

2.1 Combined thermoelasticity and photoelasticity

The efforts of one of the two supported graduate students this year have been directed towards issues of coating development for combined thermoelasticity and

photoelasticity. To review this effort, which is the heart of a related STTR, the objective is to develop a method of determining full-field measurements of the stress tensor on the surface of an in-service structure. The determination is done by combining two existing methods of stress analysis: reflection photoelasticity and thermoelasticity. Each of these methods responds to stress (as indicated by strain) on the surface of a structure, but neither is complete by itself. The missing information associated with each technique is provided by the other, so the two measurement methods are, in principal, complementary. Each of the methods depends on a coating: a birefringent coating for photoelasticity and an emissivity-enhancing coating for thermoelasticity. The critical factor in combining the methods into an NDE technique is to formulate a coating which is suitable for both methods. If the coating furthermore can act as a protective coating, it can serve as the service–protection coating for the structure as well as the diagnostic NDE coating. The effort being undertaken within this project has been associated with a search for an optimum coating and determination of an appropriate coating application method.

Most commercial photoelastic coatings are opaque and highly absorbing (as contrasted with reflecting) in the infrared band from 8-12 microns in wavelength. The most effective thermoelastic measurement system uses array technology with parallel processing, and infrared sensing arrays are generally available with sensitivity in the 3-5 micron band. Many polymeric materials which absorb in the 8-12 micron band are less absorbing or even transparent in the 3-5 micron band. For one effective approach to producing a single dual-use coating, the coating must be transparent to visible light and opaque to infrared radiation. Thus, the task being undertaken is a dual one: to find an appropriate polymer and to produce a convenient and effective method of applying it to the surface under test. To a large extent, the success achieved in developing the coating will determine the eventual marketability of the resulting technology. This factor has been considered important enough that, along with the availability of a graduate student at the appropriate stage of her academic career (Ms. Johnson), the effort in this direction has been considered appropriate for pursuit under this grant.

Along with application techniques, a variety of polymers have been examined as preliminary choices for a possible thermoelastic-photoelastic coating. These have been found with the aid Dr. Catherine Fay, a National Research Council Postdoctoral Fellow at the Polymers Branch of NASA Langley Research Center and Professor Floyd Klavetter, of the Applied Science Department of William and Mary. Besides the commercially available photoelastic coating, a Bisphenol-A based epoxy resin, films received for evaluation include, by common name, LaRC-1A, Kapton HA, UPILEX R, LaRC 8515, TOR, Kapton HY, teflon, mylar, Upilex 5 and LaRC-1Ax. Each of these materials exhibits some birefringence. The samples varied in color

from clear to a brownish-orange, in visible light optical transmission from transparent to opaque, and in thickness from 25 to 75 microns. Because of their chemical structure, the materials were expected to be opaque in the infrared, but tests in the 3-5 micron band showed them to be generally transparent. This transparency should be able to be alleviated with the addition of different chemicals to the formulation. From qualitative initial tests, Kapton HA, TOR and Upilex 5 showed the greatest birefringence of the ten films when stressed. The commercial photoelastic coating seems to be both opaque in the 3-5 micron band but also has substantial birefringence. Thus, it seems to be the best of the candidates tested. In phase 2, further searches will be made for coatings, and quantitative determinations of the strain-optic coefficient will be developed and applied.

Parallel work on the combination of thermoelastic and photoelastic stress analysis has been ongoing in England, at two universities, The University of Sheffield, under the direction of Dr Eann Patterson and the University of Liverpool, under the direction of Dr. Janice Dulieu-Smith. The Applied Science Department at William and Mary was pleased to attract Dr. Dulieu-Smith for a seminar, at which she presented several of her thoughts in exchange for a demonstration of the thermoelastic capability at the College. In addition, we were able to share information with collaborators and recent graduates of Dr Patterson's research team at a meeting of the Society of Experimental Mechanics in Nashville.

2.2 Thermoelasticity

Acceptance of a new technique in the industrial sector frequently requires a concerted, long-term effort in communication as well as simply innovation. This requirement seems to apply to thermoelastic stress analysis, and one of the major impediments to industrial application has been the time required to make a measurement. As rapid measurement is one of the hallmarks of the Stress Photonics DeltaTherm 1000 system, developed under SBIR support in conjunction with NESB at LaRC, one method of communicating and establishing credibility for the technique was begun in November 1993 by participation in a workshop in Ft. Worth, Texas, entitled "Nontraditional Methods of Sensing Damage in Materials and Structures," under the auspices of the American Society of Testing and Materials (ASTM). In part because of the success of this presentation, an invitation was received to participate in a symposium on May 20 of this year in Orlando, Florida, entitled Symposium on Nontraditional Methods of Sensing Stress, Strain, and Damage in Materials and Structures. One paper was prepared and another collaborated in: "An Array Measurement System for Thermoelastic Stress Analysis,"

and "Stress Intensity Measurement via Infrared Focal Plane Array," Both of these presentations were chosen to be considered, following peer review, for inclusion in a Special Technical Publication (STP) of ASTM. The two manuscripts are appended to this report, and they are both in the final stage of editorial review following peer acceptance. The inclusion of these two papers in a publication on ASTM is expected to support the credibility of TSA as an industrially accepted "new technique" and, in the process, provide well-deserved recognition to the NASA-supported efforts to develop this NDE measurement tool.

2.3 Thermography/Temperature Measurement

In previous years, a temperature measurement analysis was done for a situation in which a thermocouple probe was moved to a variety of positions for the purpose of obtaining a temperature profile. In particular, the temperature profile was used as a method of locating a particular feature observed on the profile - that is, as a position marker. Previously, in conjunction with another research group within NASA Langley Research Center the the Air Force Liaison Officer, a discrepancy was observed between such a marker and a radiographic position measurement. This discrepancy occurred in a Bridgman furnace used for crystal growth, and its cause and resolution were reported in the appropriate literature. The resolution involved a conduction correction to position in temperature sensors mounted on probes, a situation which can reasonably affect measurement in many instances outside of crystal growth furnaces. In order to reach this audience effectively, a presentation was made at the 42nd International Instrumentation Symposium of the Instrument Society of America entitled "Displacement Compensation of Temperature Probe Data." The presentation is available in reprint form from the proceedings of the symposium. A preprint is attached as an appendix.

An interesting application of infrared thermography was presented to the Applied Science Department by the Colonial Williamsburg Foundation (CWF) regarding industrial hazard evaluation. Each year in the autumn, CWF constructs a colonial era brick kiln to fire the bricks which have been made during the year by historically accurate interpreters of the building trades and visitors under their guidance. Operation of the brick kiln and other facilities in the historic recreation must conform to modern standards of safety, a departure from strict historical accuracy which is strongly supported by the Foundation and its visitors. As part of the continual search for safety verification, the safety officer for CWF asked for an independent evaluation of the radiation hazard to employees and visitors from operation of the kiln, which involves exposure to the mouths of the wood-fired

furnaces which are built into the kiln for a period of about 1 week. While theoretical indications and intuitive opinions from several experts in radiation have uniformly been that no hazard exists, a measurement program was undertaken to determine the heat flux from the mouths of the furnaces as a double-check the indications.

2.4 OSEE

An activity of several years with the National Center for Manufacturing Science (NMCS) was brought to a close with a final report entitled, "Investigation of the Use of Optically Stimulated Electron Emission (OSEE) to Measure Contamination Levels on Printed Circuit Boards." This report marked the first attempt started to investigate the use of OSEE for an industrial process in cooperation with representatives of the potential user industry. It indicated clearly that some of the industry-supplied substrate/contaminant pairs were easily detectable using OSEE while others were not. The project has become a prototype for similar projects in its employment of user-supplied samples and the production of points on a dose-response curve as tools in determination of applicability. The final report is included as an appendix.

A major project within the engineering development group in NESB at NASA LaRC over the period of this project has been development of a hand-held one inch footprint OSEE sensor suitable for application in an industrial setting, sometimes referred to as "on the shop floor." In the proposal for the present effort, it was presumed that this sensor would be completed and delivered prior to the start to the grant and that the only requirement would be to provide consultation on the application of the instrument. As it turned out, the instrument was not ready for demonstration until June of the grant year, and the consultation included some initial laboratory testing and preparation of a demonstration sample for cleanliness, as demonstrated with high OSEE readings corroborated with surface appearance. Further work was done with the engineering team to define the flow of argon into the lamp and measurement regions in order to accomplish a consistent reading while still conserving argon. Following a successful demonstration of the instrument in a video conference with users and supporters at NASA Marshall Space Flight Center and Thiokol Corporation, it was discovered that the lamp had little long-term stability and a short service life. These problems have moved the delivery date up, and consultation with the engineering staff continues. At the time of this report, the development of this instrument is still in its finishing stages. The woking prototype instrument is anticapated in a matter of weeks.

During the year and following the completion of all of the work required for the

project with NCMS, the (old) laboratory apparatus for performing OSEE measurements was transferred by loan to the College of William and Mary, where it has been put back into operation. It is being used in conjunction with some College-supported research into OSEE response in increasing vacuum. A summer (Research Opportunities for Undergraduates) investigator, Ryan MacAllister, learned about OSEE and performed some studies of the effect of exposure to ambient air on stainless steel samples. This determination was in support of the design of sample handling apparatus. He also helped in the design of an OSEE instrument capable of performing measurements in a vacuum. A rising senior, Bon Woo Lee, is also using the apparatus in his Senior Research Project, which includes obtaining the first vacuum measurements for the OSEE device and, in the process, bringing a new vacuum system into operation.

2.5 Scintillator Characterization

The supported student (M. West) in this activity presented a paper with his principal research results to the American Physical Society March Meeting in St Louis, Missouri. The paper was entitled "Time evolution of radiation-induced luminescence in terbium-doped silicate glass". An abstract of the presentation is included in the appendix. Mr. West successfully defended his dissertation in 1997.

2.6 References and papers presented

Johnson, D. F., D. B. Opie, H. E. Schone, M. T. Langan and J. C. Stevens, "High–Temperature Superconduction Magnetic Shields Formed by Deep Drawing," *IEEE Trans. on Applied Superconductivity* 6(1), pp. 50-54, March, 1996 (reprint attached)

Lesniak, J. R., D. J. Bazile, B. R. Boyce, M. J. Zickel, K. E. Cramer and C. S. Welch, "Stress Intensity Measurement via Infrared Focal Plane Array," *Nontraditional Methods of Sensing Stress, Strain, and Damage in Maerials and Structures, ASTM STP 1318*, George F. Lucas and David A. Stubbs, Eds., 208-220, American Society for Testing and Materials, 1997.

Welch, Christopher S., James A. Hubert and Patrick G. Barber, "Displacement Compensation of Terperature Probe Data," *Proceedings of the 42nd International Instrumentation Symposium, Instrument Society of America,*

May 5-9, 1996, San Diego, CA., pp. 225-234. (preprint attached)

Welch, C. S., Cramer, K. E., Lesniak, J. R., and Boyce, B. R. "An Array Measurement System for Thermoelastic Stress Analysis," *Nontraditional Methods of Sensing Stress, Strain, and Damage in Maerials and Structures, ASTM STP 1318*, George F. Lucas and David A. Stubbs, Eds., 198-207, American Society for Testing and Materials, 1997.

West, Michael S. and William P. Winfree, "Time Evolution of Radiation-Induced Luminescence in Terbium-Doped Silicate Glass," presented at the March Meeting of the American Physical Society, St. Louis, MO, March, 1996. (abstract attached)

3 Related Work

The work covered in this report was one of several related efforts which were mutually supportive in the Applied Science Department at the College of William and Mary. To illustrate the synergy, a brief description of the other efforts is included below.

3.1 Combined photoelastic and thermoelastic measurements

During the year roughly equivalent to this grant, the College of William and Mary was associated with a commercial firm, Stress Photonics, Inc., of Madison, Wisconsin, in Phase I of an STTR entitled "A Stress Imager Integrating Thermoelastic and Photoelastic Stress Analysis." The work at the College of William and Mary was directed towards the development of a dual-purpose easily applied coating material which could be used both for reflection photoelastic measurements and for thermoelastic measurements. As part of this work, some temperature-based methods were shown to be sensitive to thickness variations of the coatings in the range of interest Also shown was a sensitivity to photoelastic strain variations at sub-fringe levels, paving the way for thin photoelastic coating applications and delicate measurements. A Phase II proposal was written jointly by the collaborators, and it has been announced as selected, so when arrangements have been made, the work is expected to continue for the next two years.

3.2 Proposal to NSF for OSEE high-sensitivity process study

In the proposal for the work included in this report, it was noted that a proposal was under consideration at NSF to support a program examining in detail the process which causes OSEE to be very sensitive to some contaminants at very high sensitivity when the contamination amount is very small. This process has been hypothesized to be related to the change of work function on a contaminated surface, and changes in work function with contamination have been demonstrated for particular cases. However, it seems that experiments of the requisite delicacy to investigate the processes directly require a correlation with high vacuum surface inspection techniques, such as ultraviolet photoelectron spectroscopy, and support for the equipment required for such an undertaking has not been developed within the existing community of OSEE researchers and sponsors. The NSF review was completed during the project year, and the proposed effort was turned down, in part because of the size of the budget request. In turning the proposal down, some of the anonymous peer reviewers commented that the proposed research area was interesting and potentially important. A letter of support was also obtained from an interested industrial potential user of OSEE measurements. In view of the interest shown in the review of the project, the effort to characterize the high-sensitivity OSEE process is continuing, and appropriate sponsorship continues to be sought.

3.3 OSEE demonstration and evaluation

The support of OSEE technology has included efforts to broaden the base of users in order to develop a commercial market large enough to support a viable and responsive producer. The most effective technique for gaining access to industrial potential users has been demonstration projects modeled on the NCMS project originally undertaken by NASA. A project of this nature has recently been established between the College of William and Mary and Edison Welding Institute, of Columbus, Ohio. Inquiries have also been made in conversations with the president of Photoemission Technology, holders of the fundamental patent for OSEE as an NDE tool, and a verbal agreement has been made in principle to license the patent rights on a case-by-case basis for a nominal fee for activities in which OSEE technology is being demonstrated to or evaluated for potential new users.

3.4 Space Grant Fellowship

D. Johnson successfully competed for a Space Grant Graduate Fellowship during the year of this grant. Her research proposal was based on the combination of

photoelasticity and thermoelasticity, and it clearly was associated with the effort under this grant. As part of the fellowship, she took part in a video presentation prepared by the Virginia Space Grant Consortium and Old Dominion University. This presentation, entitled Journey into Cyberspace, is aimed at secondary school students of both genders to interest them in science as a career. She also produced and gave a demonstration of combined thermoelasticity and photoelasticity in conjunction with a reception for the Virginia Space Grant Consortium.

3.5 Thermographic issues demonstration and development

A thermographic and thermoelastic apparatus has been loaned to the Applied Science Department of the College of William and Mary, and it is being used for teaching and research purposes. Thermography is routinely introduced in a laboratory setting to the students taking the general NDE class. It is also being used for outreach and demonstrations to classes in primary and secondary schools in the area. Continuing a practice initiated in former years, D. Johnson has introduced students to infrared thermography in a middle school of Henrico County,

4. Summary

The work carried out under this grant has carried forward research in several efforts related to nondestructive evaluation of surfaces and thin coatings. These have been generally related to the disciplines of optically stimulated electron emission (OSEE) and combined thermoelastic and photoelastic stress analysis as a tool in nondestructive evaluation. A by-product has been a deeper understanding of the operation of common thermocouple and thermistor probes. Associated work has been done in understanding X-Ray scintillator materials and magnetic shield fabrication and evaluation using high-temperature superconducting materials. The work has been mutually supporting with other work, and a related development of commercial technology is underway in two areas.

High-Temperature Superconducting Magnetic Shields Formed by Deep Drawing

Deonna F. Johnson, David B. Opie, Harlan E. Schone, Michael T. Lanagan, and Jonathan C. Stevens

Abstract— **A new method for the construction of high-temperature superconducting magnetic shielding structures has been demonstrated. With this process, a ceramic laminate of high-temperature superconducting powder and silver metal sheets is formed and then shaped into a cylindrical magnetic shield by deep drawing before being sintered. Two types of superconducting powders were used in this experiment, $YBa_2Cu_3O_7$ and $Bi_{1.8}Pb_{0.4}Sr_2Ca_2Cu_3O_x$, which exhibited shielding factors of 1100 and 330, respectively.**

I. Introduction

MAGNETIC SHIELDING determines the measurement sensitivity, measurement resolution, or the strength of perturbations from magnetic fluctuations for many applications where isolation from ambient fields are needed. Such applications include atomic frequency standards, superconducting quantum interference device (SQUID) magnetometer systems for biomagnetic measurement systems, geomagnetism, magnetic anomaly detection, and nondestructive evaluation/testing (NDE/NDT). We have demonstrated a new process for producing large high-temperature superconducting (HTS) magnetic shielding structures which are appropriate for these applications.

HTS magnetic shields have been produced and tested by several groups [1]–[6]. The production of these shields has focused on two methods: shields formed as bulk ceramic pieces and as thick films on suitable substrates. The formation of bulk ceramic shields requires pressing of the HTS powder into the desired shape and then sintering the pressed piece. The resulting ceramic shields are susceptible to cracking during handling or temperature cycling. Thick film techniques form layers of superconductor on substrates and rely on the substrate for mechanical strength. For the yttrium-based superconductors, there are only a few substrate materials that do not produce detrimental chemical reactions with the superconductor: pure silver, silver-plated stainless steel, polycrystalline yttria-stabilized zirconia, and polycrystalline magnesium oxide. Although successful as substrates, each of these materials has its specific difficulty in the construction of magnetic shields. Zirconia and polycrystalline MgO are extremely hard ceramics and cannot be easily modified after firing to include necessary features like screw holes, mounting points, and apertures. Silver-plated stainless steel is easier to use as a substrate, but, as with all thick film shields, there are exposed HTS surfaces which can degrade during handling or exposure to humidity or condensation [7].

To circumvent these technical issues, we have demonstrated the feasibility of shields constructed from metal/HTS-powder/metal composite sheets. These sheets are deep drawn to form a shielding structure by a process similar to that used to make aluminum beverage cans. The flow of the ceramic powder with the metal during forming is critical for maintaining a continuous layer of HTS material between the silver. This process can be described as a two-dimensional analogy of the powder-in-tube method for making superconducting wires, where a large diameter tube of silver metal is filled with HTS powder and then drawn into a long filament [8]. Our method takes a composite made of two sheets of silver separated by HTS powder and deep draws it into a cylinder before sintering. Itoh *et al.* [4] also used deep drawing in the their construction of magnetic shields. Their shields were fabricated from alternately stacked NbTi and Cu sheets interleaved with Nb. The multilayer composite was then hot rolled, cold rolled, and heat treated before being deep drawn into a cylindrical shield. They found that five concentrically stacked 1-mm thick cylinders could reduce an external field of 3 T to less than 1 mT.

II. Experimental Procedure

A. Substrate Preparation

Sheets of 99.999% silver foil with a thickness of 0.5 mm were cut into various sized circular disks depending upon the specifications of the cup to be drawn. Typical cups drawn for testing were 25-mm tall with a 25-mm diameter, which required a 56-mm diameter blank. Before the superconducting powder was deposited, the silver blanks were thoroughly cleaned with acetone and heated for fifteen minutes at 400°C to anneal the silver and to clean the surface.

Two different types of superconducting powders were used in the development of these shields. The first magnetic shields were made with commercially available orthorhombic $YBa_2Cu_3O_7$, (YBCO), with an average particle size between 2 and 6 μm.[1] Electrophoresis, an established method for

Manuscript received September 29, 1995; revised January 11, 1996. This work was supported by the U.S. Army Space and Strategic Defense Command through an ARPA TRP SBIR Award under Contract DASG60-94-C-0087.

D. F. Johnson, H. E. Schone, and J. C. Stevens are with the Department of Physics, College of William and Mary, Williamsburg, VA 23187 USA.

D. B. Opie was with Physical Sciences Inc., Alexandria, VA 22314 USA. He is now with Ethicon Endo-Surgery, a Johnson and Johnson Company, Cincinnati, OH 45242 USA.

M. T. Lanagan is with the Energy Technology Division, Argonne National Laboratory, Argonne, IL 60439-8438 USA.

Publisher Item Identifier S 1051-8223(96)03010-2.

[1] Purchased through Seattle Specialty Inc.

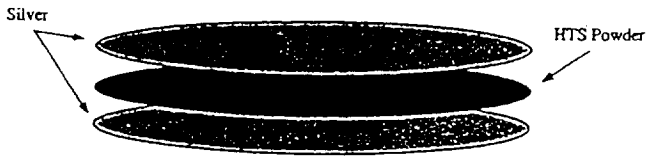

Fig. 1. A silver/HTS-powder/silver composite made from 0.5-mm silver foil plus 100 μm of HTS powder.

depositing powders in a liquid medium by an applied electric field [9], was used to deposit YBCO on the silver substrate. The deposition of $Bi_{1.8}Pb_{0.4}Sr_2Ca_2Cu_3O_x$ (BSCCO), a lead-doped mixture of 2212, Ca_2CuO_3, and CuO,[2] could not be preformed using electrophoresis because the mixture would separate during deposition. Application of BSCCO to the silver substrate was done through suspending the powder in 1-Butanol and relying on the surface tension of the butanol to hold the suspension on the substrate. The butanol evaporated and left a layer of BSCCO. These methods permitted us to vary the thickness of the HTS layers deposited on each substrate. For results shown in this paper, the thickness of the HTS layer on each silver substrate was 50 μm. Once the individual silver disks were coated with HTS powder, a silver/HTS-powder/silver composite sandwich was assembled with a total powder layer of 100 μm (Fig. 1). This flat composite was then drawn into a cylindrical magnetic shielding structure.

B. Deep Drawing

Deep drawing is a well-established process for producing thin-wall objects of relatively large heights from thin, flat sheets by imposing suitable restraining and deforming forces [10]. Cylindrical (cup-shaped) superconducting magnetic shields, the simplest shape produced by this process, are constructed by deep drawing the silver/HTS-powder/silver composites. To form a cylindrical cup from a flat blank, the blank is laid on a die which has a round hole in the center. A punch descends axially through the hole which forces the blank over the rounded edge of the die (Fig. 2). For the draw to be successful, the metal must flow smoothly to avoid longitudinal folds, or wrinkles, in the walls. The success of the deep drawing process is due to the existence of tangential compressive and radial tensile stresses that produce favorable conditions for deformation. The magnitude of the tensile stress produced must be less than the ultimate tensile strength of the material.

For tall structures, it is seldom possible to produce a finished workpiece in one draw. Several redraws are frequently necessary. In order to draw full-sized cups, we fabricated a double-action press with a hydropneumatic die cushion system to apply a controllable force on the blankholder that holds the outer periphery of the blank flat and prevents wrinkling during the draw. Although very ductile, high-purity silver does not draw well because it rapidly work-hardens. The work-hardening causes wrinkles that frequently form about midway through the draw. Prevention of these wrinkles has been the greatest difficulty encountered. Another problem with silver is its extremely low tensile strength: 120–170 MPa when fully annealed. Any nicks or irregularities can cause localized stresses to exceed the tensile strength of the material and lead to the rupture of the shield wall.

[2] Supplied by Argonne National Laboratory.

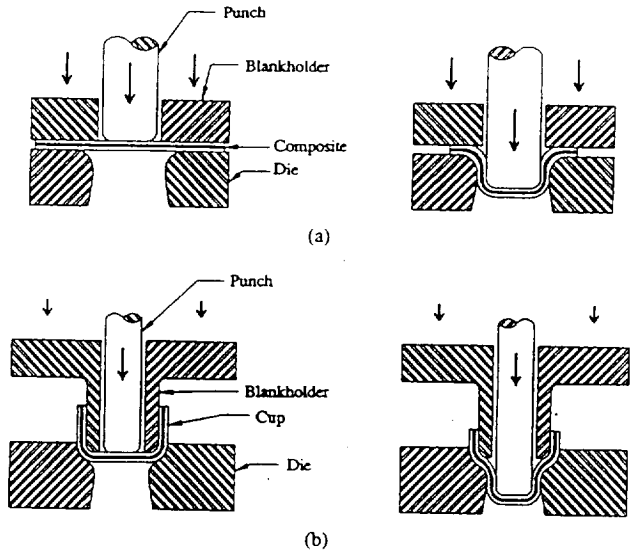

Fig. 2. Schematic cross section of the (a) draw and (b) redraw in the formation of cylindrical magnetic shields using deep drawing.

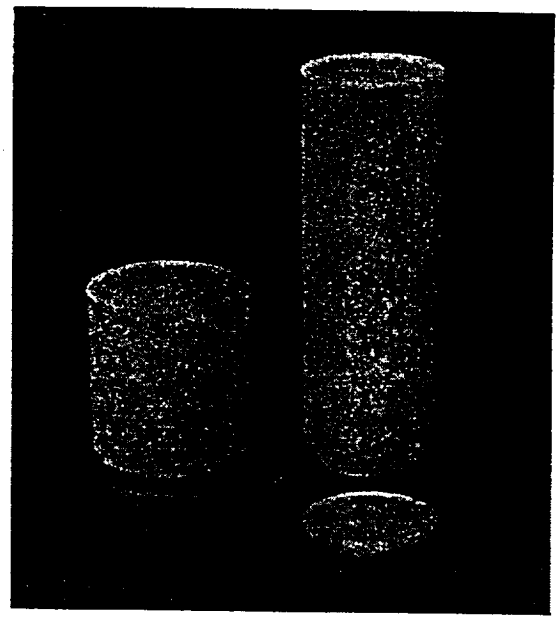

Fig. 3. Cylindrical HTS magnetic shields formed by deep drawing.

C. Cup Sintering

The shields were sintered once the mechanical shaping was complete (Fig. 3). The YBCO magnetic shields were sintered in an oxygen atmosphere at 910°C for 24 hours. Sintering temperatures higher than this were difficult due to the lowered melting temperature of silver in an oxygen atmosphere. The cooling rate was 5°C/h from 910–860°C, 60°C/h from 860–510°C, and 5°/h from 510–200°C. The BSCCO magnetic shields were sintered using a method developed for the two-powder process designed for rapid formation

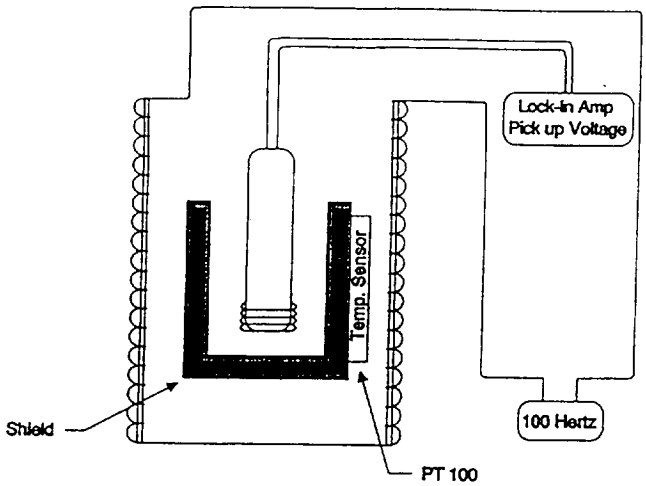

Fig. 4. Schematic cross section of the experimental setup used for measuring the transition temperature and determining the shielding factor for the magnetic shields.

of bismuth-2223 during powder-in-tube processing [11]. The BSCCO shields sintered in flowing air for 50 h at 845°C and again for 100 h after a redraw, which corresponded to a 10% reduction in the diameter of the magnetic shield. This mechanical deformation of the magnetic shield provided the alignment of grains in the BSCCO ceramic, which improved the connectivity between the conduction planes of the individual grains.

III. Characterization and Results

A. Shielding Measurements

The first characterization of the HTS magnetic shields measured the penetrated magnetic field strength along the axis of the cup. After zero field cooling to liquid nitrogen temperatures, the shields were placed in an ac magnetic field produced by a solenoid with a field strength ranging from 5 to 50 μT. The field inside of the shield was detected with a thin coil connected to a lock-in amplifier. This coil could move along the axis of the magnetic shield to measure the shielding as a function of depth along the axis of the shield (Fig. 4). A graph of shielding versus depth was constructed for each cup (Fig. 5). In this graph the top and bottom of the cup shows regions of increased signal which are attributed to flux leakage. The flux leaks into the shield from two sources: the open top of the cylinder and the closed bottom of the shield since the demagnetization factor of the corners of the right cylinder increases the local current density beyond the critical value. These measurements were made on magnetic shields that were 25-mm tall, implying that taller shields would have a significantly decreased field value in the middle of the shield far from the sources of flux leakage.

B. Measurement of T_c

By attaching a platinum resistor (PT100) to the side of the shield, we measured the transition temperature of the HTS shield. For this measurement, the shield was placed in

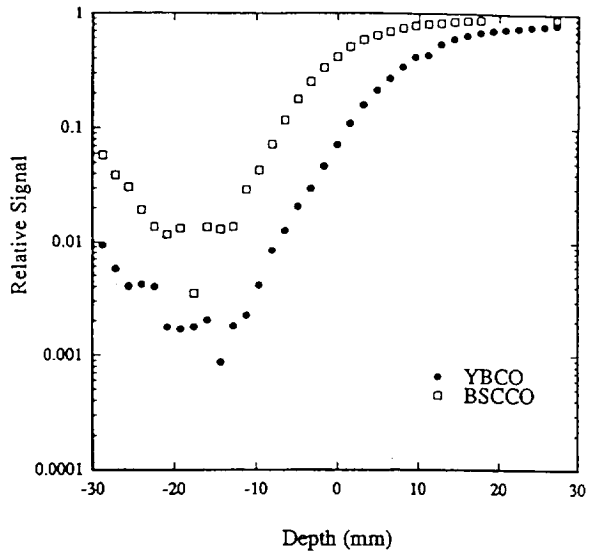

Fig. 5. Penetrated magnetic field strength measured along the axis of the shield with the top of the shield corresponding to a depth of 0 mm. The increased signal at the bottom of the shield is due to flux leakage resulting from the increased current density in this area.

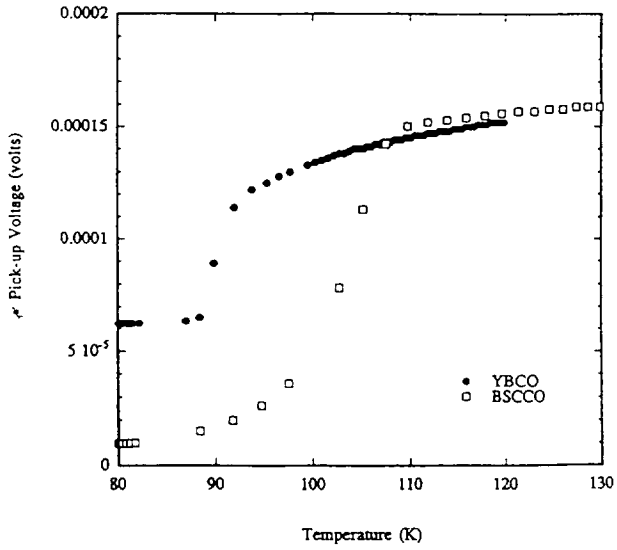

Fig. 6. Transition temperature for a BSCCO and YBCO magnetic shield. The transition temperature is 110 K for BSCCO and 92 K for YBCO.

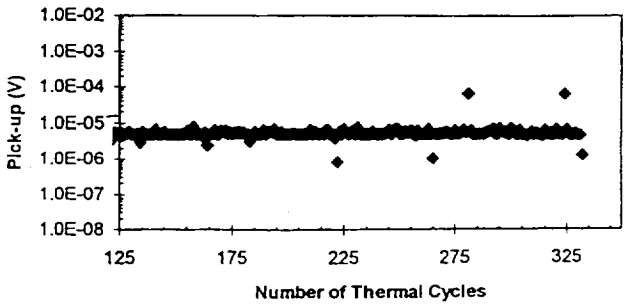

Fig. 7. Plot of pick-up voltage as a function of number of thermal cycles for a YBCO magnetic shield. The shielding factor for this measurement is greater than 1000.

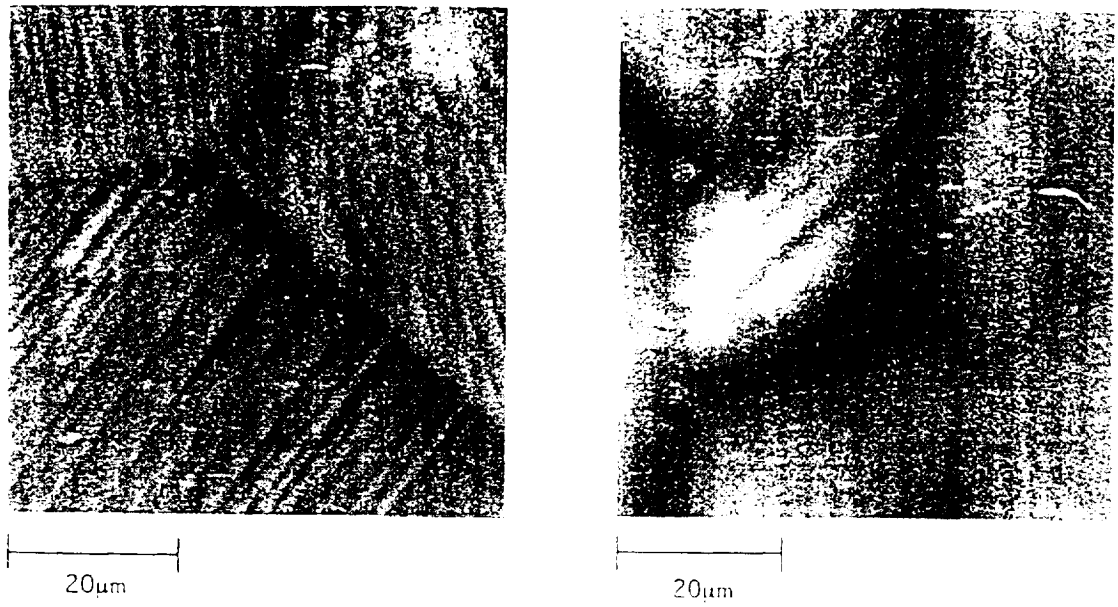

(a) (b)

Fig. 6. These photos show the 60 μm × 60 μm AFM [illegible] and [illegible] pure [illegible]. The [illegible] shows smaller grains with impurities.

a solenoid with the detection coil in the location of highest shielding. The shield was allowed to warm up and the transition temperature was recorded. This is shown in Fig. 6. We found that the BSCCO magnetic shields had a transition temperature of 110 K while YBCO shields had a transition temperature at 92 K. This is consistent with our expectations for these HTS materials.

We separated the silver layers of the already sintered shields to expose the HTS ceramic and investigated the phases present using X-ray diffraction. Comparing our samples with reference X-ray patterns confirmed that we had reached the correct superconducting phase of the material.

C. Shielding Factor

The shielding factor for the magnetic shields was determined by the ratio of signal from the inner coil without the magnetic shield present to the minimum signal with the shield

$$\text{shielding factor} = \frac{\text{signal without shield}}{\text{signal with shield}}$$

The best shielding factors recorded to date were 1100 for YBCO and 330 for BSCCO. It is important to note that researchers use different definitions of shielding factors depending upon their experimental method. This leads to various quoted values for shielding factors. Therefore, the absolute values of shielding factors from different papers are not comparable [12].

IV. Discussion

We have demonstrated a new method for the construction of high-temperature superconducting magnetic shields through deep drawing. This method has several advantages over competing processes. First, there are no exposed HTS surfaces to degrade with handling, humidity, or condensation. Furthermore, these shields may be easily modified for screw holes and other common construction features. Finally, deep drawing is a common industrial technique that we have shown to work with metal, ceramic laminates. Although the magnetic shields for this experiment were 25-mm tall with a 25-mm diameter, shields three times the height and diameter were drawn. Wrinkling is a limiting factor in the production of these larger shields because it interferes with the continuity of the HTS powder. Better process control in the drawing operation, together with a larger press, would enable the formation of larger shields.

The thermal cycling performance of the magnetic shield is a critical characteristic for practical application. We found that both the YBCO and BSCCO magnetic shields thermal cycled well. Fig. 7 shows good thermal cycling characteristics for a YBCO shield which exhibited a shielding factor of 1100.

Although the superconductor was sealed between silver layers, there does not seem to be any evidence that YBCO or BSCCO was stoichiometrically oxygen deficient. This is due to the fact that silver at the high sintering temperatures, 845 °C for BSCCO and 910 °C for YBCO, is transparent to oxygen. We also found that the quality of silver correlated with the shielding properties of the YBCO shields since YBCO is highly sensitive to oxygen content. Shields formed with 99.9% pure silver had a lower T_c than shields made from 99.999% silver. Examination of the quality of silver with an atomic force microscope showed that the 99.9% silver had a significant reduction in grain growth and a noticeable amount of impurities at the grain boundaries (Fig. 8). We conclude that this concentration of impurities inhibits the oxygen from reaching the superconducting powder, thereby contributing to the poor shielding found from using the 99.9% silver with YBCO.

ACKNOWLEDGMENT

The authors wish to acknowledge the contributions to this work from S. Remillard and L. J. Klempter, Illinois Superconductor; Profs. M. Hinders and D. Manos, Department of Applied Science, College of William and Mary; Dr. J. Bensel, Physics Department, College of William and Mary; and T. V. Prather, Physical Sciences, Inc.

REFERENCES

[1] K. Hoshino, H. Ohta, E. Sudoh, K. Katoh, S. Yamazaki, H. Takayama, H. Takahara, and M. Aono, "Magnetic shield of high-Tc Bi-Pb-Sr-Ca-Cu-O superconductors at 77K for SQUID measurements," *IEEE Trans. Magn.*, vol. 27, pp. 2202–2205, 1991.

[2] G. J. Cui, S. G. Wang, H. M. Jiang, J. Z. Li, C. Y. Li, C. D. Lin, R. Z. Liu, Q. L. Zheng, Y. S. Fu, Z. L. Luo, and W. C. Qiao, "A superconductive shielding can for high Tc SQUID," *IEEE Trans. Magn.*, vol. 25, pp. 2273–2275, 1989.

[3] M. Itoh, H. Ishigaki, and T. Ohyama, "Effect of Ag on magnetic shield of superconducting Y-Ba-Cu-O cylinders," *Cryogenics*, vol. 30, pp. 863–867, 1990.

[4] I. Itoh, T. Sasaki, S. Minamino, and T. Shimizu, "Magnetic shielding properties of NbTi/Nb/Cu multilayer composite tubes," *IEEE Trans. Appl. Superconduct.*, vol. 3, pp. 177–180, 1993.

[5] J. O. Willis, M. E. McHenry, M. P. Maley, and H. Sheinberg, "Magnetic shielding by superconducting Y-Ba-Cu-O hollow cylinders," *IEEE Trans. Magn.*, vol. 25, pp. 2502–2505, 1989.

[6] M. M. Miller, T. Carroll, R. Soulen, Jr., L. Toth, R. Rayne, N. McN. Alford, and C. S. Saunders, "Magnetic shielding and noise spectrum measurement of Y-Ba-Cu-O and (Bi,Pb)-Sr-Ca-Cu-O superconducting tubes," *Cryogenics*, vol. 33, pp. 180–183, 1993.

[7] D. B. Opie, "Advanced composite laminates for forming high temperature superconducting magnetic shields," Physical Sciences, Inc., Alexandria, VA, Phase I SBIR Final Rep., Contract DASG60-94-C-0087, 1995.

[8] D. Y. Kaufman, M. T. Lanagan, S. E. Dorris, J. T. Dawley, I. D. Bloom, M. C. Hash, N. Chen, M. R. DeGuire, and R. B. Poeppel, "Thermomechanical processing of reactively sintered Ag-Clad $(Bi,Pb)_2Sr_2Ca_2Cu_3O_x$ tapes," *Appl. Superconduct.*, vol. 1, pp. 81–91, 1993.

[9] B. Zhang, P. Fabbricatore, G. Gemme, R. Musenich, R. Parodi, and L. Risso, "Preparation and characterization of $YBa_2Cu_3O_{7-x}$ superconducting films deposited by electrophoresis," *Physica C*, vol. 193, pp. 1–7, 1992.

[10] AMS Int., *Metals Handbook, 14, Forming and Forging*, Metals Park, OH, 1988.

[11] S. E. Dorris, B. C. Prorok, M. T. Lanagan, S. Sinha, and R. B. Poeppel, "Synthesis of highly pure bismuth-2223 by two-powder process," *Physica C*, vol. 212, pp. 66–74, 1993.

[12] J. Wang and M. Sayer, "High temperature superconductors for low frequency magnetic shielding," *IEEE Trans. Appl. Superconduct.*, vol. 3, pp. 185–188, 1993.

Deonna F. Johnson received the B.S. degree in physics from Bethany College, Bethany, WV, in 1992, and received the M.S. degree from the College of William and Mary, Williamsburg, VA, in December 1994.

She is currently a physics Ph.D. candidate at the College of William and Mary, where she is working in the field of nondestructive evaluation focusing on the application of thermoelasticity.

David B. Opie received the B.A. degree in physics from the University of Delaware, Newark, in June 1986. He received the M.S. degree in June 1988 and the Ph.D. degree in December 1991, both from the College of William and Mary, Williamsburg, VA.

While at William and Mary, his research was directed toward the development of a compact hydrogen maser frequency standard and applications of high-temperature superconductivity. From 1991 to 1995, he was with Physical Sciences Inc., Alexandria, VA. His research interests were focused on the applications of high-temperature superconductors, compact frequency standards, and nondestructive evaluation. Currently, he is a Principal Scientist at Ethicon Endo-Surgery, a Johnson and Johnson Company. His research interests are directed toward applying electromagnetic, ultrasonic, and laser technology to the development of medical devices.

Harlan E. Schone received the B.S. degree in engineering physics from the University of Illinois, Urbana, and the Ph.D. degree in physics from the University of California, Berkeley, in 1961.

He was employed at Boeing Research Lab from 1961 to 1965 and has been on the faculty at the College of William and Mary, Williamsburg, VA, since 1965. He has worked in the area of electronic properties of metals using NMR and muon spin rotation techniques. Recent work has involved studies of the effect of hydrogen on the electronic properties of high-temperature superconductors.

Michael T. Lanagan received the B.S. degree in ceramic engineering from the University of Illinois, Urbana, and the Ph.D. degree from Penn State University, University Park.

At Penn State, he studied the microwave dielectric properties of ferroelectric and antiferroelectric materials. He joined Argonne National Laboratory in 1987, where he presently explores the electrical and mechanical properties of high-temperature superconductors. His work encompasses synthesis and fabrication of superconductors, fuel cells, and dielectric ceramics. In addition, he has been with IBM and Corning Glass. He has authored or coauthored over 100 publications in the field of electronic ceramics.

Jonathan C. Stevens received the B.S. degree in computer science from the College of William and Mary, Williamsburg, VA, in 1993.

He is currently working as an independent designer of electronic and mechanical equipment for material testing. He developed the drawing techniques for this work.

Displacement Compensation of Temperature Probe Data

Christopher S. Welch
Senior Research Scientist
Applied Science Department
College of William and Mary
Williamsburg, VA 23187

James A. Hubert
6780 Deer Bluff Drive
Dayton, Ohio 45424

Patrick G. Barber
Professor and Co-director of Chemistry
Department of Natural Sciences
Longwood College
Farmville, VA 23909

KEYWORDS

Temperature Probe Measurement, Conductivity Error, Displacement Compensation, Temperature Profile Measurement

ABSTRACT

Analysis of temperature data from a probe in a vertical Bridgman furnace growing germanium crystals revealed a displacement of the temperature profile due to conduction error. A theoretical analysis shows that the displacement compensation is independent of local temperature gradient. A displacement compensation value should become a standard characteristic of temperature probes used for temperature profile measurements.

TEMPERATURE PROBE COMPENSATION

When temperature probes are used to measure the temperature of surrounding fluids, liquids, or gases, corrections are frequently made to the raw temperature data. These corrections are intended to account for rapid temporal and spatial changes of the environmental temperature, direct heating of the probe through absorption of radiation, and conductive heat loss through the structure supporting the sensitive element. For each of these corrections, formulas have been developed over the years

and are available in handbooks so that practitioners can have access to ready guidance. For thermocouple measurements a reference such as Moffatt [1962] is among those available. In general, these formulas provide correction values of temperature to be applied at the position ascribed to the sensitive element of the probe. This paper reports another interpretation which applies a correction to the position, rather than the temperature, of the sensitive element. In some cases, a displacement correction is more intuitive and somewhat simpler than the temperature correction.

DISCREPANCY BETWEEN RADIOGRAPHIC AND TEMPERATURE PROBE MEASUREMENTS

The motivation for this work came from an experiment in which the position of the melt-solid interface in a vertical Bridgman furnace used for the growth of germanium crystals was estimated by two independent methods: x-ray radiography and temperature profile measurements from a thermocouple probe. The objective of the experiment was to verify whether thermocouple measurements could be used to monitor crystal growth.

The furnace consisted of two nearly isothermal sections maintained at approximately 1100 K in the lower section and 1270 K in the upper section. The temperatures of these two sections bracketed the 1210 K melting point of germanium. With this furnace configuration the melt-solid interface can be kept in the 3 cm region between the isothermal zones during most of the growth. A schematic diagram of the experimental setup is shown in Figure 1.

Because the solid and liquid phases of germanium differ in density by 4%, the melt-solid boundary could be measured using x-ray radiography. Measurements were made from radiographic images on film, and the boundary location was estimated by measuring the position of the interface with respect to fixed objects which provided fiducial locations on the film. One of the features visible on the film is the tip of the thermocouple probe, providing a verification of the position measurement of the probe.

The temperatures were measured using a thermocouple which moved inside a centerline capillary tube. The capillary tube was fabricated as part of the sample ampule [Hubert, *et al*, 1993]. Because the thermal conductivity of the liquid and crystalline phases of germanium differ, the interface location could be estimated using a plot of the temperature vs position data obtained by the thermocouple in the centerline capillary. The location of the interface was postulated as the point at which the slope of the temperature versus position data changes. This assumes that heat flux is primarily axial in the cylindrical germanium sample and continuous through the interface. The

difference in thermal conductivity requires a compensating difference in temperature gradient to maintain continuity in the heat flux. In the measured data, the sharp break in temperature gradient was smoothed by conduction effects, so the position was determined as the intersection of two straight lines fit by least squares to the data on either side of the approximate position.

The positions of the melt-solid interface determined radiographically and thermally differed systematically by 3 mm, The melt-solid interface determined from the thermal data was 3 mm into the liquid zone as determined by the x-ray measurements.

NUMERICAL MODEL OF PROBE TIP TEMPERATURE

Hubert [1992] constructed a series of numerical models to evaluate the radiation environment and thermal flow in the entire furnace, including the thermocouple probes. These models were designed and run to represent varying locations of the thermocouples found in the experimental data. The results verified the experimental observation that the temperature profile measured at the thermocouple tip is shifted 3 mm toward the liquid zone. The results also showed that the heat flow through the sample is generally axial near the insulating region of the furnace. This result along with the axial symmetry of the experiment allow a good approximation of the thermocouple temperature end-effects to be obtained through one-dimensional analysis.

MATHEMATICAL ANALYSIS LEADING TO DISPLACEMENT INTERPRETATION

The formula given by Moffatt [1962] for correction of conduction error in thermocouples used to measure temperatures in gas streams is

$$T_T - T_J = (T_T - T_M)/\cosh[L(4h_c/d\,k_S)^{1/2}] \qquad (1).$$

In this equation, T_T represents the true temperature of the flowing gas stream being sampled by the thermocouple, which is considered as extending into the stream from a wall of the experimental chamber or model surface. T_J is the temperature of the thermocouple junction, so the left side of the equation corresponds to the conduction error. T_M is the temperature of the mount for the thermocouple, or the chamber wall. L is the length of the thermocouple junction, h_c is the coefficient of thermal transfer between the junction and the surrounding gas, and k_S is the thermal conductivity of the junction along the length of the wires. One way to visualize the thermocouple

described by this equation is as a long cylinder of length, L, much greater than its diameter, d, extending from a flat mount with the junction temperature represented by the temperature at the terminal end of the cylinder. Equation (1) can be derived from a one-dimensional analysis of the conductive heat equation on such a structure if the heat flux through the top of the cylinder is neglected and the gas surrounding the cylinder is considered to be isothermal with a constant thermal transfer coefficient.

The argument of the hyperbolic cosine in Eq. 1 contains many of the physical parameters which determine the amount of conduction error. As the product of L, which has dimensions of (length)^1 and the factor within the square root, must be dimensionless, the factor within the square root must have dimensions of (length)$^{-2}$. The inverse of this factor can be interpreted as a product of two terms, each having the dimension of (length)^1. As noted by Moffatt [1962], one of these, d/4, represents the ratio of the area of a cross-section of the cylinder to its perimeter. The value of this factor can clearly be altered by choosing different junction cross-sections, so the factor forms a useful design parameter. The other factor, k_s/h_c, is the ratio of the axial thermal conductivity of the junction to its heat transfer coefficient. This factor has dimensions of (length)^1. The square root of the product of these factors occurs so often in the analysis that we choose to give it a separate symbol, Λ, and treat it as the major parameter of the analysis,

$$\Lambda = [(w/p)(k_s/h_c)]^{1/2}, \qquad (2)$$

where w and p denote respectively the area and perimeter of the cross section. In this form, the argument of the hyperbolic cosine in Eq. 1 becomes (L/Λ), the ratio of the junction length to a characteristic length.

To adapt this analysis to the environment of the Bridgman furnace, the most important addition is a temperature gradient along the length of the probe. The one-dimensional heat equation is then

$$T''(x) - (1/\Lambda^2)T(x) = -(a/\Lambda^2)x, \qquad (3)$$

as given in Carslaw and Jaeger [1959]. The new parameter, a, denotes the thermal gradient of the surroundings. If the cylindrical rod carrying the thermocouple is considered to extend from negative infinity to x=0 and the ambient temperature scale is set to zero at x=0, , the solution is given as

$$T(x) = ax - a\Lambda \exp(x/\Lambda), \quad (x<0). \qquad (4)$$

At the tip (x=0), the temperature of the surroundings is zero, but that of the probe tip is -aΛ. This happens to be the temperature of the surroundings at location x=-Λ, so one can interpret the difference as a temperature difference at the probe tip or alternately as a displacement difference of the measurement location. If the displacement interpretation is chosen, the correction needed does not depend on the value of the thermal gradient, a value which is not available prior to the measurement.

CORRECTION TO DATA FROM THE BRIDGMAN FURNACE

The Bridgman furnace provides an example which illustrates the difference between adjusting for conduction in a thermocouple through a temperature correction and through a displacement. The data are simulated for a material with exactly a two-to-one ratio of thermal conductivities for the melt and solid phases respectively. Hubert [1992] solved the linear heat equation for the temperature profile in a probe passing through the interface in this case. For a probe entering from the cold region, the tip temperature is given by

$$T_J(x) = a\,(x - \Lambda),\ \text{for } x < 0 \qquad (5)$$

and

$$T_J(x) = (a\,x/2) - (a\,\Lambda/2)\,(1 + \exp(-x/\Lambda)),\ \text{for } x > 0, \qquad (6)$$

where $T_J(x)$ denotes the tip temperature for a probe with its tip at location x, the distance above the interface. Equations (5) and (6) are plotted as circles in Fig. 2a and 2b for an example probe having a value for Λ of 2 mm, and the heat flow is chosen to produce exactly a 1 degree/mm gradient in the solid phase and 0.5 degree/mm gradient in the liquid phase. The temperature of the material in this idealization is represented by the solid lines. The change in slope of the probe temperatures is seen to occur approximately 2 mm into the liquid phase of the material.

If a temperature correction is applied to these data, the correction is dependent of the slope of the data. The data on either side of the observed change in slope can be corrected by the corresponding amount and are represented by triangles in Figure 2a. As shown, the data between the actual interface and the observed change in slope cannot be properly corrected. Also, the data near the observed change in slope cannot easily be used due to the curvature present. If linear curve fits are applied to the remainder of the data, the approximate location of the actual interface can be found. However, this process requires estimation of the slope of the data twice, which induces additional error into the correction, and it cannot use all the available data.

The alternative is simply to apply the displacement correction Λ to the entire data set, thereby shifting the curve appropriately. Figure 2b shows the same material

temperature and measured values as figure 2a. The squares represent the displacement correction of Λ (2 mm) towards the solid region. This simple, uniform correction is independent of the particular data, and its accuracy is given by the thermocouple and environmental properties. The displacement correction automatically produces an appropriate correction for the conduction error associated with the measured temperature values.

EXPERIMENTAL VERIFICATION

Barber, *et al* [1996] performed an experiment in which a thermocouple was used to measure the temperature profile in a Bridgman furnace compared with a radiographically determined phase interface with the thermocouple inserted from both the cold zone and the hot zone of the furnace along a centerline capillary. The two temperature profiles, shown in Figure 3, were displaced from one another by about 11 mm. The temperature error at the melt point was 5 K for the probe coming from the hot zone and 16 K for the probe entering from the cold zone. The breaks in the two sets of lines differed in temperature by only 3 K. The midpoint between the two breaks in the the lines fell within one degree K of the melt point of germanium and within 2 mm of the interface as determined from x–radiography. This finding agrees substantially with the one-dimensional theoretical analysis. In this experiment, type R thermocouples were used which have a significantly larger displacement correction parameter, Λ, than the type K thermocouples used to obtain the data reported by Hubert [1992]. As a further test of the hypothesis that conduction error manifested in an end effect was responsible for the spatial offset between the radiographically determined interface and that determined by probe measurements, Barber, *et al.*[1996] constructed a type "R" (Pt - Pt/10%Rhodium) thermocouple with one leg extending from the hot region of the furnace and the other one extending from the cold region. The measured break in the curves occurred well within 1 K of the melt point and slightly more than 1 mm from the radiographically measured interface. The remaining spatial offset may be attributable to the difference in thermal conductivities of the two thermocouple materials, the alloyed platinum having slightly less than half the thermal conductivity of the pure platinum.

CONCLUSION AND RECOMMENDATION

We conclude that conductivity error leads to a spatial offset in temperature profile data taken with the thermocouple probe in the Bridgman furnace experiments. Because the error arose from causes unrelated to the specifics of the particular environment, we conclude that spatial offset is a general feature of temperature profile data obtained with

probes. We recommend that the offset parameter, A, become a standard, reported characteristic of temperature probes which are intended for use in temperature profiling measurements.

ACKNOWLEDGEMENTS

The authors acknowledge the support of Archibald Fripp, Jr., who provided intellectual guidance, laboratory facilities, and some financial support through NASA Grant NAG-1-627 to one of the authors (P.G.B). Another author (C.S.W.) was supported in part by NASA Grant NAG-1-1585 and its successors. Willard Bauserman, of NASA, shared unselfishly his expertise and experience in thermocouple probe measurements and techniques.

REFERENCES

1. Barber, P. G., A. L. Fripp, Jr., W. J. Debnam, Jr., G. Woodall, R. F. Berry and R. T. Simchick, "Experimental verification of agreement between thermal and real time visual melt-solid interface positions in vertical Bridgman grown germanium," *J. Crystal Growth 160*, (March, 1996),55-58.

2. Carslaw, H. S. and J. C. Jaeger, *Conduction of Heat in Solids*, 2nd ed. (Oxford University Press, Oxford, 1959), p. 134.

3. Hubert, James A. *Numerical thermal analysis of a sample of germanium with a centerline capillary tube in a vertical Bridgman Furnace*, Master's Thesis, George Washington University, Washington, DC (1992).

4. Hubert, James A., Archibald L. Fripp, Jr. and Christopher S. Welch, "Resolution of the discrepancy between temperature indicated interface and radiographically determined interface in a vertical Bridgman furnace," *Journal of Crystal Growth 131*, (1993), 75-82.

5. Moffat, R. J., "Gas Temperature Measurement," in *Temperature: Its Measurement and Control in Science and Industry, Vol. 3.*, Ed. C. M. Herzfeld, *Part 2, Applied Methods and Instruments*, Ed. A. I. Dahl, (Reinhold Publishing Corporation, New York, 1962), 553-571.

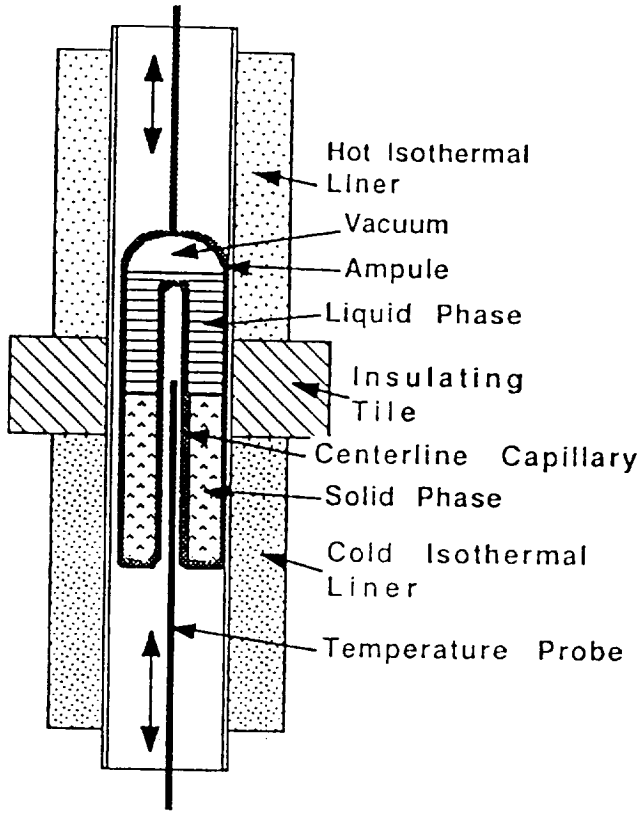

Figure 1. Schematic representation of the temperature measurement apparatus in a Bridgman furnace used to monitor crystal growth. The ampule can be moved to grow or melt the solid phase, and the temperature probe can be moved to sample different positions. The drawing is not to scale.

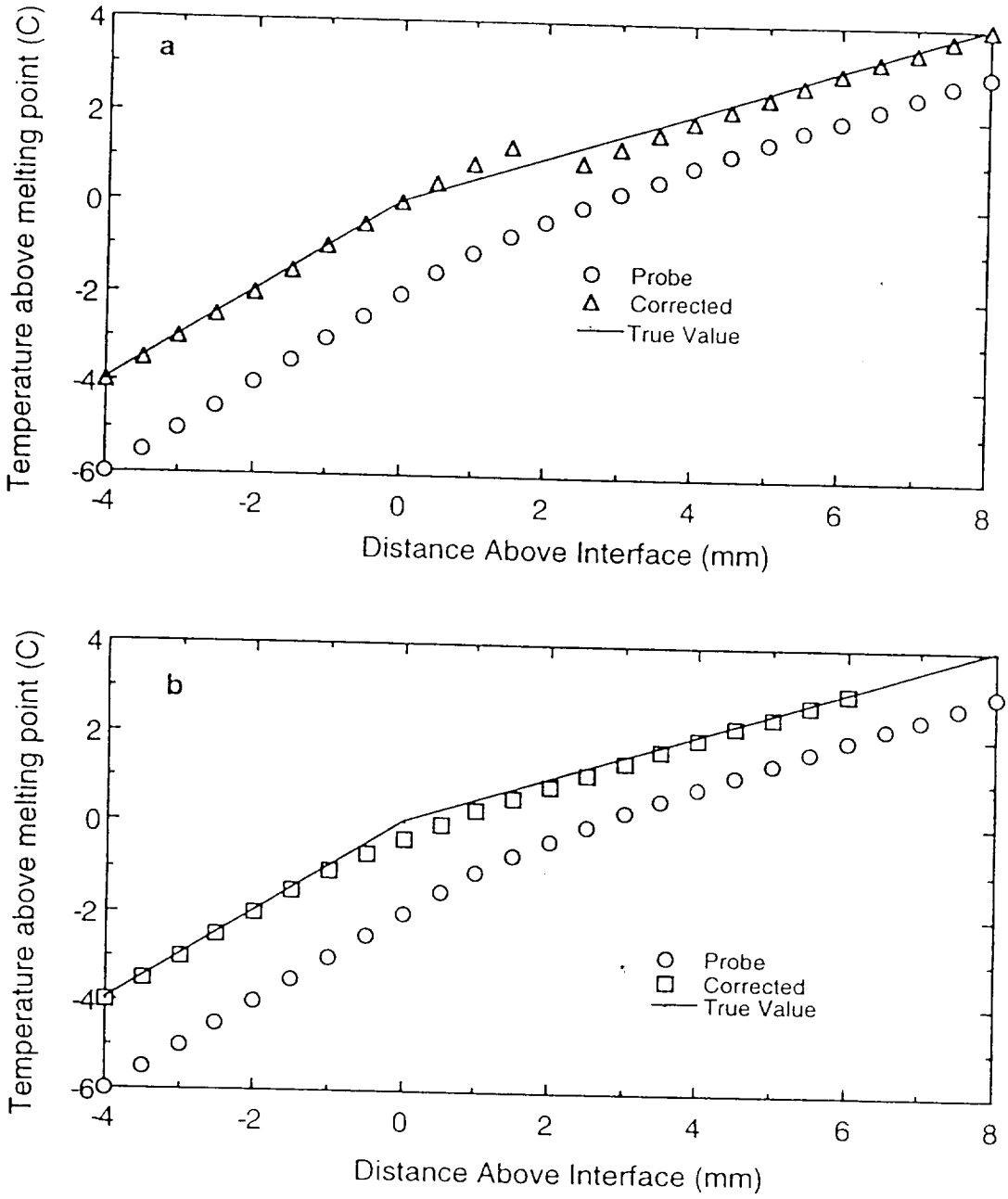

Figure 2. Example showing corrections to simulated probe data. True temperature is shown by the line segments and probe data are shown by circles. In 2a, the triangles indicate the temperature correction based on remote slopes and the apparent break in the temperature curve while in 2b, the squares indicate a displacement correction. The simulation uses idealized parameters resembling Bridgman furnace conditions.

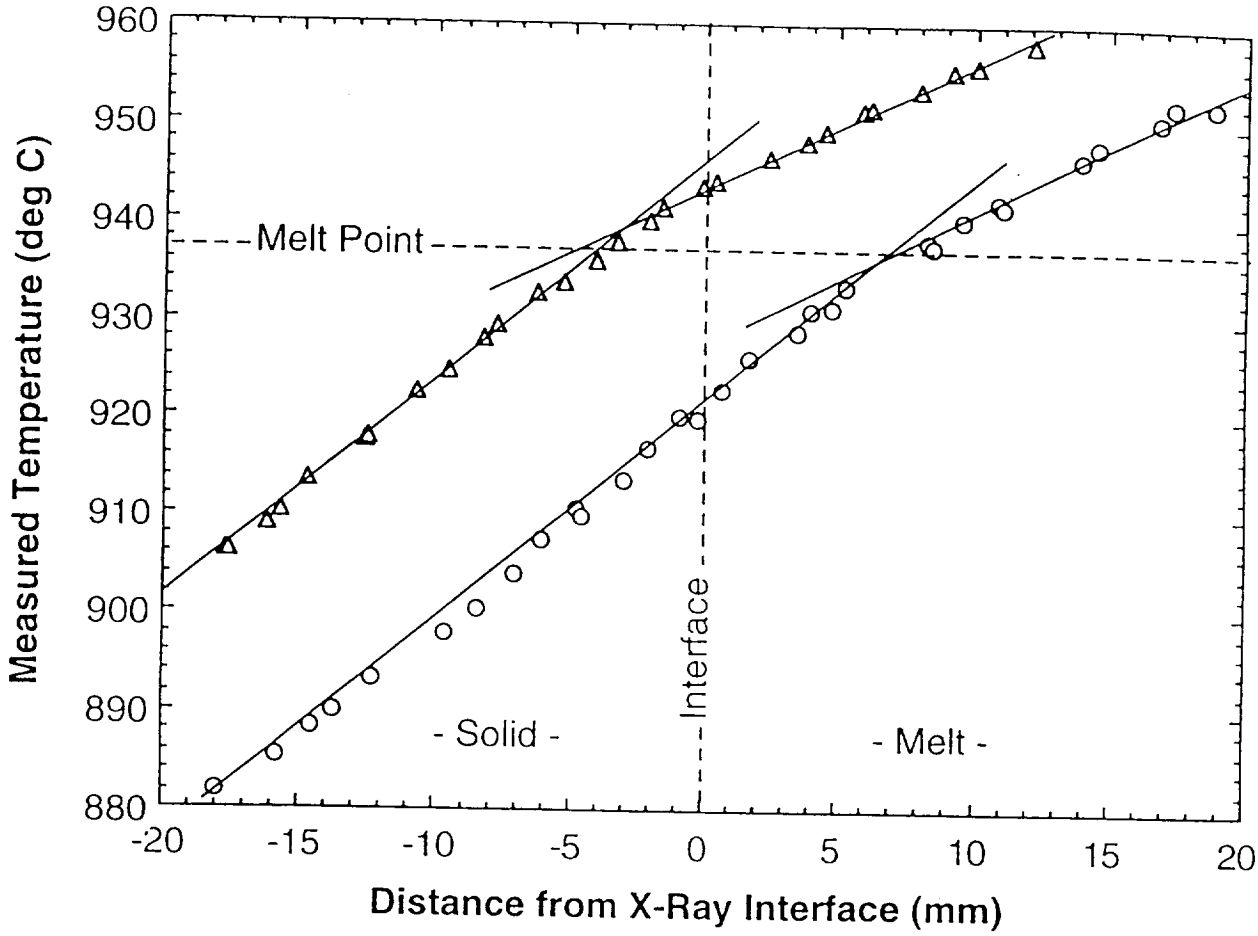

Figure 3. Temperature Profiles in a Bridgman Furnace obtained by thermocouple probes extending from the top (triangles) and bottom (circles) of a centerline capillary tube. Each measurement is made with respect to a melt-solid interface in a sample ampule containing germanium. (after Barber, *et al*, 1996)

Abstract Submitted
for the Mar96 Meeting of
The American Physical Society

Sorting Category: 16.b

Time evolution of radiation-induced luminescence in terbium-doped silicate glass MICHAEL S. WEST, The College of William & Mary, WILLIAM P. WINFREE, NASA Langley Research Center — A study was made on two commercially available terbium-doped silicate glasses. There is an increased interest in silicate glasses doped with rare-earth ions for use in high-energy particle detection and radiographic applications. These glasses are of interest due to the fact that they can be formed into small fiber sensors; a property that can be used to increase the spatial resolution of a detection system. Following absorption of radiation, the terbium ions become excited and then emit photons via 4f-4f electronic transitions as they relax back to the ground state. The lifetime of these transitions is on the order of milliseconds. A longer decay component lasting on the order of minutes has also been observed. While radiative transitions in the 4f shell of rare-earth ions are generally well understood by the Judd-Olfelt theory, the presence of a longer luminescence decay component is not. Experimental evidence that the long decay component is due, in part, to the thermal release of trapped charge carriers will be presented. In addition, a theoretical model describing the time evolution of the radiation-induced luminescence will be presented.

☐ Prefer Oral Session
☒ Prefer Poster Session

Michael West
west@physics.wm.edu
Department of Physics, The College of William & Mary

Date submitted: February 12, 1996

Electronic form version 1.1